

Long-Range ^1H – ^{19}F Distance Measurement in Peptides by Solid-State NMR

Sungsool Wi, Neeraj Sinha, and Mei Hong*

Department of Chemistry, Iowa State University, Gilman 0108, Ames, Iowa 50011

Received June 23, 2004; E-mail: mhong@iastate.edu

Solid-state NMR has been used as a unique tool for obtaining atomic-level structure of a wide variety of molecules without restrictions on morphology or molecular order. Magic-angle spinning (MAS) solid-state NMR has been successfully applied to biological samples in crystalline,¹ lyophilized,² membrane-bound,^{3,4} or fibrous⁵ states to obtain high-resolution spectra. To obtain structural restraints in unoriented proteins, the MAS-averaged anisotropic interactions such as dipolar coupling or chemical shift anisotropy (CSA) must be reintroduced by rf pulses that interfere with the spinning modulation.^{6,7} One of the most widely used recoupling techniques is rotational-echo double resonance (REDOR),^{8,9} which uses a series of π pulses spaced half a rotor period apart to recouple heteronuclear dipolar interaction between spin-1/2 nuclei. Analysis of REDOR data is routine in most cases using the simple universal curve, provided that the spin pair is well isolated, the duration of each π pulse is small compared to the rotor period, rf inhomogeneity is small or well-compensated, and the offset and CSA of nuclei in the dipolar pair are small. Various improved REDOR schemes that address these complications have been designed for low- γ nuclei.^{10–14} The REDOR distance range can be extended by incorporating high- γ ^1H or ^{19}F nuclei into the heteronuclear spin pair. For example, a 50 Hz dipolar coupling corresponds to a distance of only 3.96 Å for a ^{13}C – ^{15}N pair but 13.2 Å for a ^1H – ^{19}F pair. To measure long-range ^1H –X distances, however, couplings of the X spin to many proximal protons must be suppressed. Moreover, homonuclear couplings among protons must be disconnected. Recently, we introduced a method that achieves these by a $\text{Y}-\{^1\text{H}^{\text{Y}}-\text{X}\}$ spin assembly, where X and Y are ^{15}N or ^{13}C , $\text{Y}-^1\text{H}^{\text{Y}}$ are directly bonded, and $^1\text{H}^{\text{Y}}-\text{X}$ is the distant spin pair of interest.^{15,16} In this experiment, homonuclear ^1H decoupling is essential during $^1\text{H}^{\text{Y}}-\text{X}$ REDOR evolution, and the X-dephased ^1H magnetization is transferred selectively to the Y spin for detection by a short Lee–Goldburg cross-polarization (LG-CP) step. Fluorine has been used in REDOR experiments to extract distances up to ~ 15 Å semiquantitatively^{17,18} and has also been used to determine the orientation of membrane peptides in lipid bilayers.^{19,20} The incorporation of the sensitive ^{19}F spin as an NMR probe causes little perturbation of the native structure compared to fluorescence probes or ESR spin labels^{21,22} and has the advantage of having no natural abundance background in proteins.

In this communication, we demonstrate the first measurement of a ^1H – ^{19}F distance using REDOR and show that this long-range distance probe is useful for restraining the tertiary structure of proteins. We use as a model system a ^{19}F -labeled chemotactic peptide *N*-formyl-Met-[^{15}N , ^{13}C] Leu-[4- ^{19}F] Phe-OH (f-MLF-OH) diluted to 20% in unlabeled and protonated f-MLF-OH to minimize the effect of intermolecular couplings. The mixture has identical ^{13}C and ^{15}N chemical shifts as protonated f-MLF-OH, indicating no structure perturbation by the ^{19}F label. The fluorine of [4- ^{19}F] Phe in f-MLF-OH has an anisotropy (δ) of 50 ppm and asymmetry parameter (η) of 0.6, corresponding to a span of 33.8 kHz at 9.4 T. The choice of ^{19}F at the para position makes the $^1\text{H}_{\text{Leu}}^{\text{N}}-\text{}^{19}\text{F}_{\text{Phe}}$

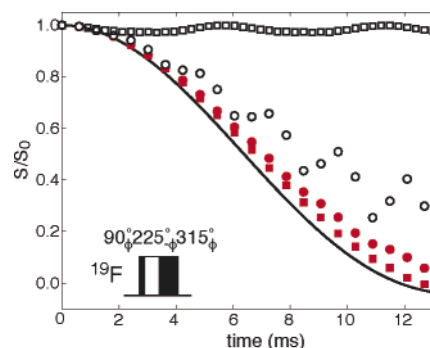


Figure 1. Numerical REDOR simulations for 120 Hz ^1H – ^{19}F coupling using ^{19}F 180° pulses (open symbols) and $90^\circ 225^\circ 315^\circ$ composite pulses (filled symbols) both with XY-16 phase cycling. Squares: 15 kHz offset and no CSA for ^{19}F . Circles: no offset and 33.8 kHz CSA span. The composite pulse compensates for the resonance offset nearly completely and the CSA effect partially. Solid line: the universal REDOR curve.

distance immune to potential phenylene ring flips. A challenge arises when a large CSA is involved in the REDOR spin pair. We used a $90^\circ 225^\circ 315^\circ$ composite pulse, originally designed to compensate for resonance offsets,²³ to reduce the detrimental effect of the large ^{19}F chemical shift on the REDOR dephasing curve.

Figure 1 shows the results of numerical simulations for 120 Hz of ^1H – ^{19}F dipolar coupling under simple ^{19}F 180° pulses versus $90^\circ 225^\circ 315^\circ$ composite pulses. REDOR with a single ^1H π pulse and multiple ^{19}F pulses was considered. A spinning speed of 3307 Hz and a ^{19}F rf field strength of 50 kHz, identical to the experimental conditions, were used in the simulations. With a 15 kHz offset and no CSA for ^{19}F , the π -pulse REDOR shows virtually no dephasing while the composite-pulse REDOR exhibits dephasing nearly identical with the universal curve, with the slight deviation due to the finite pulse length.^{10,24} With no isotropic shift offset but 33.8 kHz of CSA for ^{19}F , the composite-pulse REDOR still exhibits relatively complete and stable dephasing while the π -pulse REDOR shows oscillatory behavior. The considerable immunity of the $90^\circ 225^\circ 315^\circ$ composite-pulse REDOR over large isotropic shift offsets and CSA is confirmed experimentally (Supporting Information). The increased duty cycle of the composite pulse (34.6% of a rotor period in our experiments) causes only a minor underestimate of the dipolar frequency (Figure 1).

Figure 2a shows the experimental ^{15}N -detected $\{^1\text{H}_{\text{Leu}}^{\text{N}}-\text{}^{19}\text{F}_{\text{Phe}}\}$ REDOR control (S_0) and dephased curves (S/S_0) of the 20% diluted f-MLF-OH. The experiment used six MREV-8 cycles²⁵ per rotor period, 75 μs ^1H – ^{15}N LG-CP,²⁶ and XY-16 phase cycling for the composite pulses.¹¹ The ^1H echo signal of $^1\text{H}_{\text{Leu}}^{\text{N}}$ in the absence of the ^{19}F pulses (S_0) fits to a 3.9 ms T_2 . The S/S_0 curve, measured to 6 ms, is best fit by a coupling of 120 ± 20 Hz, which corresponds to a dipolar coupling of 255 ± 40 Hz after taking into account the MREV-8 scaling factor of 0.47.²⁵ This translates to a $^1\text{H}_{\text{Leu}}^{\text{N}}-\text{}^{19}\text{F}_{\text{Phe}}$ distance of 7.7 ± 0.4 Å, which is ~ 0.65 Å longer than the de novo solid-state NMR structure²⁷ after taking into account the increased van der Waals radius of ^{19}F . Inclusion of possible intermolecular

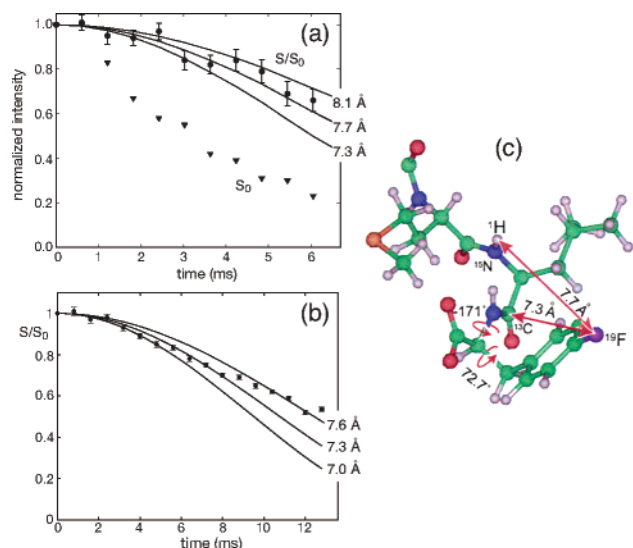


Figure 2. (a, b) $^1\text{H}^{\text{N}}\text{Leu}-^{19}\text{F}_{\text{Phe}}$ and $^{13}\text{C}'_{\text{Leu}}-^{19}\text{F}_{\text{Phe}}$ REDOR data of f-MLF-OH. (a) $^1\text{H}-^{19}\text{F}$ S/S₀ decay (circles) is best fit to 7.7 ± 0.4 Å. Triangles: ^1H S₀ decay. Simulations include the ^{19}F CSA and the ^{19}F rf field of 50 kHz. (b) $^{13}\text{C}'-^{19}\text{F}$ S/S₀ curve, best fit to 7.3 ± 0.3 Å. (c) Refined f-MLF-OH structure²⁷ based on the two distances, drawn using Insight II. Phe torsion angles ($\phi = -171^\circ$, $\chi_1 = 72.7^\circ$) were found. All NMR spectra were measured on a Bruker DSX-400 spectrometer at 9.4 T using a 4-mm MAS probe equipped with a HFX unit. A quantity of 3.5 mg of labeled f-MLF-OH was cocrystallized and diluted to 20% with unlabeled peptide from 2-propanol and was center-packed in a 4-mm rotor. Spinning speed: 3307 Hz.

$^1\text{H}-^{19}\text{F}$ distances based on the crystal structure of the related f-MLF-OMe peptide did not change the distance result beyond experimental uncertainty. A complementary $^{13}\text{C}'_{\text{Leu}}-^{19}\text{F}_{\text{Phe}}$ REDOR experiment yielded a distance of 7.3 ± 0.3 Å (Figure 2b), which is ~ 0.45 Å longer than the reported f-MLF-OH structure.²⁷

To convert the REDOR distances to torsion angles, we modified the Phe (ϕ , χ_1) angles from the reported f-MLF-OH structure (PDB id: 1q7o). Although Leu (ϕ , ψ , ω) also affects the $^1\text{H}-^{19}\text{F}$ distance, these backbone torsion angles were more precisely measured than the side chain (0.02 Å rmsd for the peptide backbone and 0.38 Å rmsd for all heavy atoms).²⁷ In particular, the Phe side chain was the least constrained in the previous structure because of the lack of ψ and χ_2 angles. Around the reported Phe (ϕ , χ_1) angles of (-166.5° , 55.7°), searching in steps of 0.1° , we found a unique angular set (-171° , 72.7°) that agrees with both the $^1\text{H}^{\text{N}}\text{Leu}-^{19}\text{F}_{\text{Phe}}$ and $^{13}\text{C}'_{\text{Leu}}-^{19}\text{F}_{\text{Phe}}$ distances. Figure 2c shows the refined f-MLF-OH structure based on the REDOR data. The angle differences between our data and the literature values are $\Delta\phi = 4.5^\circ$ and $\Delta\chi_1 = 17.0^\circ$. The $\Delta\phi$ value is within experimental uncertainty, while χ_1 at first appears to differ more significantly. However, a close examination of the previous χ_1 angle measurements by HNCH and HCCH experiments showed that two degenerate solutions of 68° and 52° were found with broad minima.²⁸ The higher value agrees well with our structure, but the lower value was slightly favored in the final structure because of excluded volume constraints.²⁷ Since the Phe ring orientation was not well-defined in the previous structure, the current REDOR-refined structure most likely falls within the ensemble of 56 975 f-MLF-OH structures reported in the previous study.²⁸ It is interesting to note that the X-ray structure of f-MLF-OMe shows $\chi_1 = 64^\circ$, which is in the middle of the two NMR solutions.

We have demonstrated heteronuclear-detected $^1\text{H}-^{19}\text{F}$ REDOR, the longest heteronuclear distance probe in solid-state NMR thus far. For the current $^1\text{H}^{\text{N}}-^{19}\text{F}$ distance, the corresponding $^{15}\text{N}-^{19}\text{F}$

distance (8.24 Å) would give a coupling of ~ 20 Hz, which would be very difficult to measure accurately. The $^1\text{H}^{\text{N}}\text{Leu}-^{19}\text{F}_{\text{Phe}}$ distance combined with the $^{13}\text{C}'_{\text{Leu}}-^{19}\text{F}_{\text{Phe}}$ distance restrained and refined the backbone ϕ and side chain χ_1 torsion angles of Phe in f-MLF-OH. Labeling of ^{19}F nuclei in proteins is feasible for a number of amino acids, such as Ala, Phe, Tyr, and is useful for restraining protein side chain structure, which may not always be available from torsion angle experiments. The maximum measurable $^1\text{H}-^{19}\text{F}$ distance depends on the ^1H T₂, which can be 5–6 ms in crystalline solids^{15,16} and may increase with improved homonuclear decoupling, possibly at higher spinning speeds, thus extending the measurable $^1\text{H}-^{19}\text{F}$ distances to ~ 10 Å. We envision that a few selective long-range $^1\text{H}-^{19}\text{F}$ distances can help restrain the global fold and the supramolecular organization of proteins, complementing more local structural parameters such as dihedral angles and short C–N distances.

Acknowledgment. This research was supported by an NSF Grant (MCB-93398) and a Sloan Research Fellowship (to M.H.). We thank Prof. Rienstra for helpful discussions of MLF structure.

Supporting Information Available: Pulse sequence, verification of broadband inversion by the $90^\circ 225^\circ 315^\circ$ pulse, and effect of potential intermolecular couplings on the REDOR curve. This material is available free of charge via the Internet at <http://pubs.acs.org>.

References

- (1) Igumenova, T.; McDermott, A.; Zilm, K.; Martin, R.; Paulson, E.; Wand, A. *J. Am. Chem. Soc.* **2004**, *126*, 6720–6727.
- (2) Goetz, J. M.; Poliks, B.; Studelska, D. R.; Fischer, M.; Kugelbrey, K.; Bacher, A.; Cushman, M.; Schaefer, J. *J. Am. Chem. Soc.* **1999**, *121*, 7500–7508.
- (3) Grobner, G.; Burnett, I. J.; Glaubitz, C.; Choi, G.; Mason, A. J.; Watts, A. *Nature* **2000**, *405*, 810–813.
- (4) Lansing, J. C.; Hu, J. G. G.; Belenky, M.; Griffin, R. G.; Herzfeld, J. *Biochemistry* **2003**, *42*, 3586–3593.
- (5) Tycko, R. *Annu. Rev. Phys. Chem.* **2001**, *52*, 575–606.
- (6) Dusold, S.; Sebald, A. *Annu. Rep. NMR Spectrosc.* **2000**, *41*, 184–264.
- (7) Bennett, A. E.; Griffin, R. G.; Vega, S. In *NMR Basic Principles and Progress*; Springer-Verlag: Berlin, 1994; Vol. 33, pp 3–77.
- (8) Gullion, T.; Schaefer, J. *J. Magn. Reson.* **1989**, *81*, 196–200.
- (9) Gullion, T.; Schaefer, J. *J. Magn. Reson.* **1991**, *92*, 439–442.
- (10) Jaroniec, C. P.; Tounge, B. A.; Rienstra, C. M.; Herzfeld, J.; Griffin, R. G. *J. Magn. Reson.* **2000**, *146*, 132–139.
- (11) Gullion, T. *Concepts Magn. Reson.* **1998**, *10*, 277–289.
- (12) Sinha, N.; Schmidt-Rohr, K.; Hong, M. *J. Magn. Reson.* **2004**, *168*, 358–365.
- (13) Chan, J. C. C.; Eckert, H. *J. Magn. Reson.* **2000**, *147*, 170–178.
- (14) Weldeghiorghis, T. K.; Schaefer, J. *J. Magn. Reson.* **2003**, *165*, 230–236.
- (15) Schmidt-Rohr, K.; Hong, M. *J. Am. Chem. Soc.* **2003**, *125*, 5648–5649.
- (16) Sinha, N.; Hong, M. *Chem. Phys. Lett.* **2003**, *380*, 742–748.
- (17) Toke, O.; Maloy, W. L.; Kim, S. J.; Blazyk, J.; Schaefer, J. *Biophys. J.* **2004**, *87*, 662–674.
- (18) McDowell, L. M.; Studelska, D. R.; Poliks, B.; O'Connor, R. D.; Schaefer, J. *Biochemistry* **2004**, *43*, 6606–6611.
- (19) Glaser, R. W.; Sachse, C.; Dürr, U. H. N.; Wadhvani, P.; Ulrich, A. S. *J. Magn. Reson.* **2004**, *168*, 153–163.
- (20) Afonin, S.; Dürr, U. H. N.; Glaser, R. W.; Ulrich, A. S. *Magn. Reson. Chem.* **2004**, *42*, 195–203.
- (21) Afonin, S.; Glaser, R. W.; Berditchevskaya, M.; Wadhvani, P.; Gührs, K.-H.; Möllmann, U.; Perner, A.; Ulrich, A. S. *ChemBioChem* **2003**, *4*, 1151–1163.
- (22) Grage, S. L.; Salgado, J.; Dürr, U.; Afonin, S.; Glaser, R. W.; Ulrich, A. S. In *Perspectives on Solid State NMR in Biology*; Kiihne, S. R., de Groot, H. J. M., Eds.; Kluwer Academic Publishers: Dordrecht, The Netherlands, 2001; Vol. 1, pp 83–91.
- (23) Starcuk, Z.; Sklenar, V. *J. Magn. Reson.* **1985**, *62*, 113–122.
- (24) Schmidt, A.; Vega, S. *Isr. J. Chem.* **1992**, *32*, 215–230.
- (25) Rhim, W. K.; Elleman, D. D.; Vaughan, R. W. *J. Chem. Phys.* **1973**, *59*, 3740–3749.
- (26) van Rossum, B. J.; de Groot, C. P.; Ladizhansky, V.; Vega, S.; de Groot, H. J. M. *J. Am. Chem. Soc.* **2000**, *122*, 3465–3472.
- (27) Rienstra, C. M.; Tucker-Kellogg, L.; Jaroniec, C. P.; Howhy, M.; Reif, B.; McMahon, M. T.; Tidor, B.; Lozano-Pérez, T.; Griffin, R. G. *Proc. Natl. Acad. Sci. U.S.A.* **2002**, *99*, 10260–10265.
- (28) Rienstra, C. M.; Hohwy, M.; Mueller, L. J.; Jaroniec, C. P.; Reif, B.; Griffin, R. G. *J. Am. Chem. Soc.* **2002**, *124*, 11908–11922.

JA0462732